

Accretion Disk Instabilities

F. Meyer

Max-Planck-Institut für Physik und Astrophysik
Institut für Astrophysik
Karl-Schwarzschild-Str. 1
D-8046 Garching bei München, FRG

I. Introduction

In this article we discuss two instabilities of stationary accretion disks which lead to an understanding of observed light variations in accretion disk systems, the dwarf novae and the rapid burster MXB 17030-335. The accretion disks in these systems avoid instability at the cost of stationarity and perform stable cycles in which sudden changes of the accretion flow lead to corresponding, often dramatic, variations of their accretion luminosity.

Figure 1 shows a light curve of U Geminorum. It was discovered in 1855 by J.R. Hind and has become a prototype of the dwarf novae. In these systems an extended time of quiescence of up to several weeks is followed by a short outburst of a few days during which the luminosity rises by a factor of 30 to 100. The dwarf novae belong to the cataclysmic variables. They are all close binaries in which a white dwarf primary is orbited by a Roche lobe-filling low mass secondary. Through the inner Lagrangian point mass flows over from the secondary and forms a luminous accretion disk around the white dwarf. In the case of the dwarf novae this disk has temperatures below about 10000K in its outer region. It will be discussed how partial ionization and convection then affect the vertical structure of the disk such that the stationary flow becomes unstable.

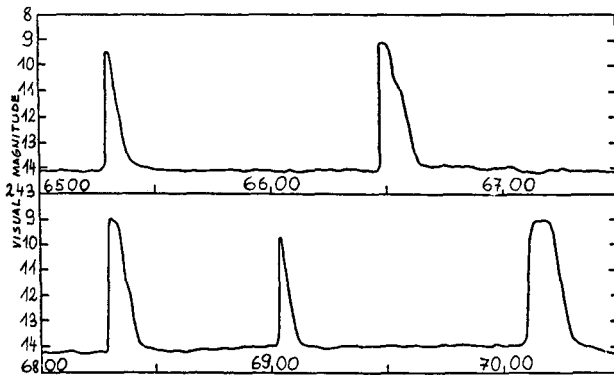


Fig. 1. Light curve of the dwarf nova U Geminorum. Abszissa in days ([2])

The second type of instability to be considered arises when the accretion disk becomes so hot that radiation pressure becomes important. It is therefore expected in the interior parts of accretion disks in X-ray binaries (for which the white dwarf

of the cataclysmic variable system is replaced by a much smaller but equally massive neutron star). We will suggest here that it is responsible for the type II X-ray outbursts, notably the "trapezoidal" bursts of the rapid burster MXB 17030-335 which is the prototype and up to now only representative of its class, discovered by Lewin et al. [3] from the SAS-3 satellite and also extensively observed from the Hakucho and Tenma satellites by Kunieda et al. [4]. Figure 2 shows the light curve of the rapid burster during 3 different phases of its activity.

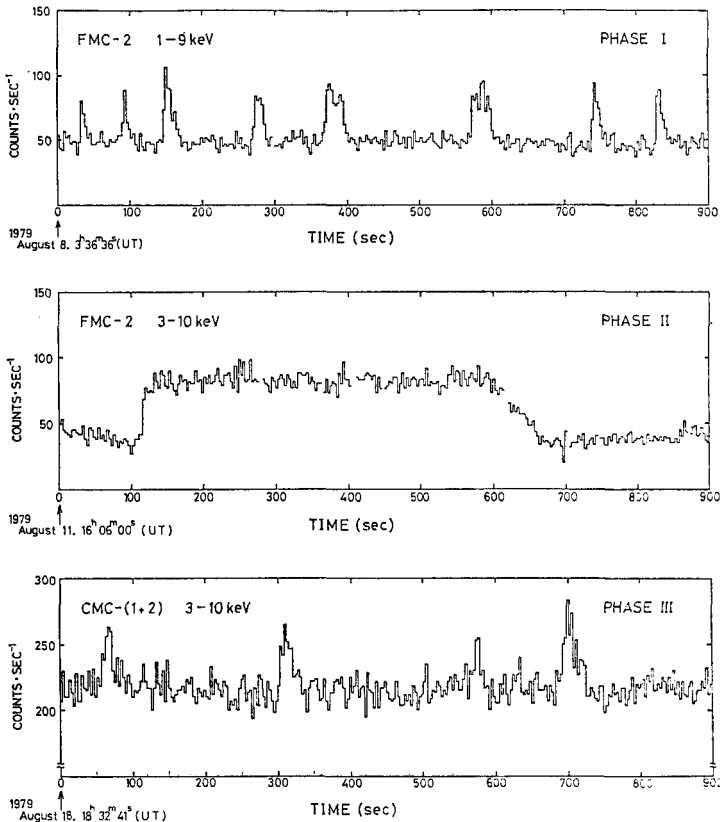


Fig. 2. X-ray light curves of MXB 17030-335 showing type II bursts in 3 different activity phases (KUNIEDA et al. [4])

How do such accretion disk instabilities lead to these two classes of phenomena? In order to show this we first give a short description of the relevant accretion disk physics. We then discuss the new features which the partial ionization-convection related instability introduces and show how it can explain the dwarf novae light cycles. We then consider the radiation pressure related Lightman-Eardley instability and discuss its dependence on the form of the frictional law assumed. In the final section we suggest that this instability triggers a transition to spherical accretion and mass loss which is capable of explaining the type II trapezoidal bursts of the rapid

burster, and discuss some interesting questions arising from this model interpretation.

II. Accretion Disk Theory

For a full description with historical references of accretion disk theory we refer the reader to Pringle's 1981 review [5]. The later discussion of the dwarf novae instability is still mostly in the original literature. First reviews were given by Smak [6] and Meyer [7].

For simplicity we consider here rotationally symmetric, non-selfgravitating and geometrically thin accretion disks. The outer regions of accretion disks in close binaries will deviate from rotational symmetry by the action of tidal forces from the companion and the stream impact of the mass overflow. These and other features of non-axially symmetric nature are excluded from consideration by the symmetry assumption. The basic instability can, however, be discussed in the simplified model. In contrast to possibly self-gravitating accretion disks around newly forming stars the disk masses in the close binary systems are of order $10^{-10} M_{\odot}$ and their own gravity can safely be neglected compared to that of the two stars. The assumption of geometrical thinness is crucial for disk theory and allows the separate treatment of the vertical and radial structures of accretion disks.

The disk thickness is measured by the scaleheight H over which the pressure decreases vertically in support of the gas against the effective vertical gravity

$$g_z = - \frac{GM}{r^2} \frac{z}{r} \quad (1)$$

where terms of order $(z/r)^2$ are neglected compared to 1 (cylindrical co-ordinates r, ϕ, z with r distance from axis and z distance from midplane, G gravitational constant and M central mass). Hydrostatic equilibrium then yields (for an isothermal gas)

$$\frac{H}{r} = \left[\frac{2R_g T r}{GM} \right]^{1/2} \approx \frac{V_s}{v_{\phi}} \quad (2)$$

(R_g gas constant including molecular weight, T midplane temperature, V_s isothermal sound velocity, v_{ϕ} azimuthal velocity). Typical values for H/r in cataclysmic variable accretion disks are $\approx 1/30$. Radial pressure gradients (V_s^2/r) are then of order $(H/r)^2$ small compared to gravity GM/r^2 and the latter must be entirely compensated by the centrifugal force of circular Kepler orbits with angular velocity

$$\Omega(r) = \left[\frac{GM}{r^3} \right]^{1/2} \quad (3)$$

In the presence of a viscosity the shear motion $d\Omega/dr \neq 0$ introduces a frictional stress

$$\tau_{r\phi} = \mu r \frac{d\Omega}{dr} \quad (4)$$

which transfers angular momentum and allows the gas to gradually spiral inward.

This process is described by the conservation equations for mass and angular momentum,

$$\frac{\partial}{\partial t} (2\pi r \Sigma) - \frac{\partial \dot{M}}{\partial r} = 0 \quad (5)$$

$$\frac{\partial}{\partial t} (2\pi r \Sigma r^2 \Omega) - \frac{\partial}{\partial r} [(\dot{M} - 3\pi f) r^2 \Omega] = 0 \quad (6)$$

where \dot{M} is the inward directed mass accretion rate, Σ is the surface density

$$\Sigma = \int_{-\infty}^{+\infty} \rho dz . \quad (7)$$

and f is the viscosity integral

$$f = \int_{-\infty}^{+\infty} \mu dz . \quad (8)$$

The second term in the square bracket is the frictional transport of angular momentum obtained from integration of (4) and use of the Kepler angular velocity (3). Elimination of M from (5) and (6) results in the well-known diffusion equation

$$\frac{\partial \Sigma}{\partial t} = \frac{3}{r} \frac{\partial}{\partial r} \left[r^{1/2} \frac{\partial}{\partial r} (r^{3/2} f) \right] . \quad (9)$$

If f is a function of only Σ (and r) one can obtain $\frac{\partial f}{\partial t}$ by multiplying with $\partial f / \partial \Sigma$. The equation thus displays the diffusion coefficient

$$D = 3 \frac{\partial f}{\partial \Sigma} . \quad (10)$$

Note that $f/\Sigma = \nu$ is a measure of the kinematic viscosity in the disk. Solutions of equation (9) are stable for $\partial f / \partial \Sigma > 0$ but unstable if $\partial f / \partial \Sigma < 0$.

What is the viscosity operating in observed accretion disks? The diffusivity ν determines the characteristic radial diffusion time

$$t_d = \frac{r^2}{\nu} . \quad (11)$$

If one inserts molecular diffusivities one finds that this estimate yields times which are by a factor up to 10^{14} too long to account for observed time changes in accretion disks (basically by a factor H/λ , where λ is the molecular mean free path). Such a small viscosity would also lead to an extreme mass accumulation within the disk and thereby effectively dam up the heat flow to the disk surfaces. This would inflate the disk rather to a rotating stellar envelope, contrary to observations.

Shakura and Sunyaev [8] and Novikov and Thorne [9] parametrized the obviously non-molecular viscosity by introducing the non-dimensional ratio α between frictional stress (equation 4) and pressure P .

$$\tau_{r\phi} = \alpha P . \quad (12)$$

Estimates in the way of (12) for dwarf novae accretion disks (BATH and PRINGLE [10] and for symbiotic stars (DUSCHL [11]) yielded values

$$10^{-2} \leq \alpha \leq 1 . \quad (13)$$

The viscosity can then be written as

$$\mu \approx \alpha \rho H v_s \quad (14)$$

(ρ density). Thus α (≤ 1) would stand for the Mach number of some turbulent exchange. Alternatively the stresses of small scale magnetic fields,

$$\tau_{r\phi} = \frac{B_r B_\phi}{4\pi} \quad (15)$$

(eg. dynamo generated) would yield α as a ratio of magnetic to gas energy

density. In any case the estimates (13) for α point to a macroscopic process for the effective friction in accretion disks.

The thermal time scale is obtained by comparing the energy density with the rate of frictional heating,

$$t_{th} \approx \frac{P}{\tau_r \phi \Omega} = \frac{1}{\alpha \Omega} . \quad (16)$$

In regions of partial ionization it is increased by some factor η (a typical value is 5) due to contributions of ionization energy to the internal energy. Except for this factor η the thermal diffusivity

$$\nu_{th} \approx H^2/t_{th} \quad (17)$$

is the same as the kinematic viscosity

$$\nu = \mu/\rho \approx H^2/t_{th} . \quad (18)$$

From (11) this yields

$$t_d \approx \left[\frac{r}{H} \right]^2 t_{th} . \quad (19)$$

the timescale for variations by radial diffusion is thus by $(r/H)^2 \approx 10^3$ large compared to that for local thermal relaxation. Since dynamical equilibrium in the vertical direction is reached on the even shorter time scale $H/V_s \approx 1/\Omega$ the disk is on such long timescales in thermal and dynamical equilibrium.

Thus the vertical structure of accretion disks is determined by the equations of hydrostatic equilibrium, radiative or convective energy transport and frictional heat generation. As in stellar structure computations one has to add an equation of state, opacity values (which enter into the thermal conductivity), and a photospheric boundary condition, for example a grey atmosphere. In optically thin disks the temperature is determined by the requirement that the frictional heat must be radiated away. In cool regions thus a state of marginal ionization is sustained which tends to act as a thermostat (WILLIAMS [12], TYLENDÁ [13]). For a discussion of the action of the Coriolis force on convection see [14].

The processes responsible for the anomalous viscosity probably introduces itself some kind of convective exchange (be it by magnetic buoyancy or by hydrodynamic instability) and thereby might influence the energy transport and the vertical structure. For radiatively layered disk regions such processes would pump heat downward (stable temperature gradient) but the resulting effect on the temperature structure is very small due to the efficiency of radiative energy transport (DUSCHL [15]). In regions unstable to thermal convection the temperature structure becomes near adiabatic and an additional source of convection only tends to decrease a small difference even more.

Solutions for the vertical disk equilibrium yield the height z_0 of the optically deep disk (or the scale height of the optical thin disk) and the energy flux density F as a function of surface density for each radial distance r ,

$$\begin{aligned} z_0 &= z_0(\Sigma, r) , \\ F &= F(\Sigma, r) , \end{aligned} \quad (20)$$

corresponding (SMAK [6]) to the mass-radius and mass-luminosity relations of main sequence stars. The accretion disk can thus be pictured as an infinite radial sequence of "plane" stars exchanging mass according to equation (9). The total

emitted energy F per unit surface area and time results from the integration of the specific heat generation by friction, $\mu(r d\Omega/dr)^2$,

$$F = \frac{9}{8} \frac{GM}{r^3} f(\Sigma, r) . \quad (21)$$

Thus (20) becomes equivalent to a viscosity-surface density relation $f(\Sigma, r)$ which allows the discussion of instabilities. In stationary accretion disks the viscosity integral f is proportional to the mass accretion rate \dot{M} , a simple consequence of the frictional dissipation of gravitational energy. For zero net angular momentum flow through the disk one has from (6)

$$\dot{M} = 3 \pi f . \quad (22)$$

If the Kepler angular momentum at the inner disk boundary $r=R$ is carried inward together with the mass a factor $(1-\sqrt{R/r})$ is to be added on the left hand side of this equation ([8]) and other factors apply to other specification of the net angular momentum flow in the disk.

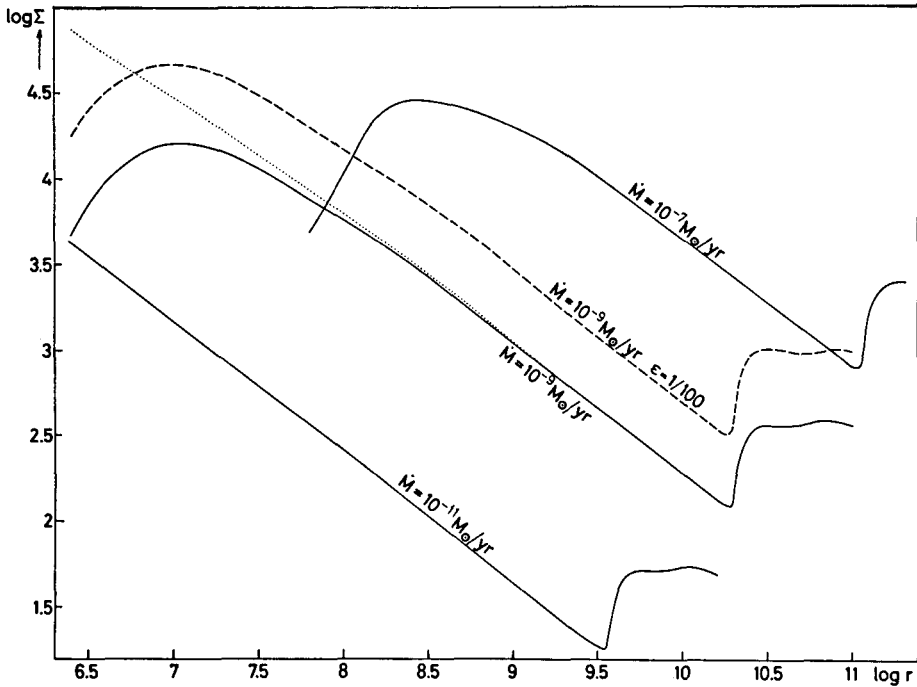


Fig. 3. Surface density Σ as function of radius r (cgs units) for different mass accretion rates \dot{M} in a stationary accretion disk around a central mass of $1 M_{\odot}$. (α parameter $\approx 1/14$) (from [14]). Dotted curve: Friction coupled to gas pressure instead of total pressure

Figure 3 shows a numerically determined disk structure in form of $\log \Sigma - \log r$

relations for different constant \dot{M} . Such results depend in particular on the assumption about the parameter α taken here as constant. The smooth decrease of surface density with radius in the middle part of this diagram is a consequence of support by gas pressure and energy transport by radiative diffusion. This behaviour ends in an abrupt density increase when the disk temperature drops below approximately 10000K. Then partial ionization strongly affects the opacity and the specific heat, and associated convection appears. This keeps the temperature at the central plane cooler and thereby decreases the frictional diffusivity. As a result the surface density increases considerably to allow the same amount of mass accretion to pass through.

This increase of surface density can lead to intersection between two curves of different \dot{M} at the same values of Σ and r . In other words, at such distance r the same value of the surface density Σ allows two different stationary mass accretion rates. We show in the next section that this feature leads to instability and disk outburst cycles involving transitions between two such states.

One further notes in Figure 3 that intersections of curves also appear in the inner disk regions. The turnover there is due to the growing importance of radiation pressure for the hydrostatic equilibrium and results in the Lightman-Eardley instability. One may note that this feature disappears when the friction in equation (12) is coupled to the gas pressure (instead of to the total pressure), as is expected for models of magnetic friction. We will show, however, that the instability can reappear for non-constant α -values.

III. The Dwarf Nova Instability

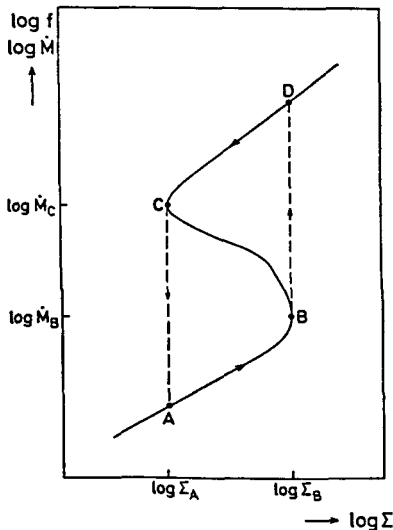


Fig. 4. Viscosity-surface density relation at $\log r = 10$ for $\alpha=1$. Ordinate compressed by a factor 2. Branch BC is unstable, for accretion rates feeding the disk between \dot{M}_B and \dot{M}_c the disk performs relaxation oscillations indicated by arrows

Figure 4 shows a viscosity-surface density relation $f(\Sigma)$ at a fixed distance r obtained from such computations. Its typical S-shape is the clue to the cyclic variations expected (see BATH and PRINGLE [16]). The ordinate is also a measure of the local mass flow rate \dot{M} (see (21)). The upper branch corresponds to radiative energy transport in a fully ionized disk. $df/d\Sigma > 0$ implies stability of the

stationary state of the disk (equation (9)). As the mass accretion rate \dot{M} decreases the accretion heated gas becomes cooler until the upper turning point at Σ_B is reached at a temperature of about 10^4 K. The onset of partial ionization and convection produces the middle branch with $df/\partial\Sigma < 0$. Disk flows with such accretion rates have no stable stationary solution. At the lower turning point at Σ_A partial ionization is ended and the gas becomes either nearly neutral and convective or optically thin. This cool lower branch is again stable. Note that the viscosity integral and the mass accretion rate also measure the effective temperature $T_{\text{eff}} = (F/\sigma)^{1/4}$ (equation (21)).

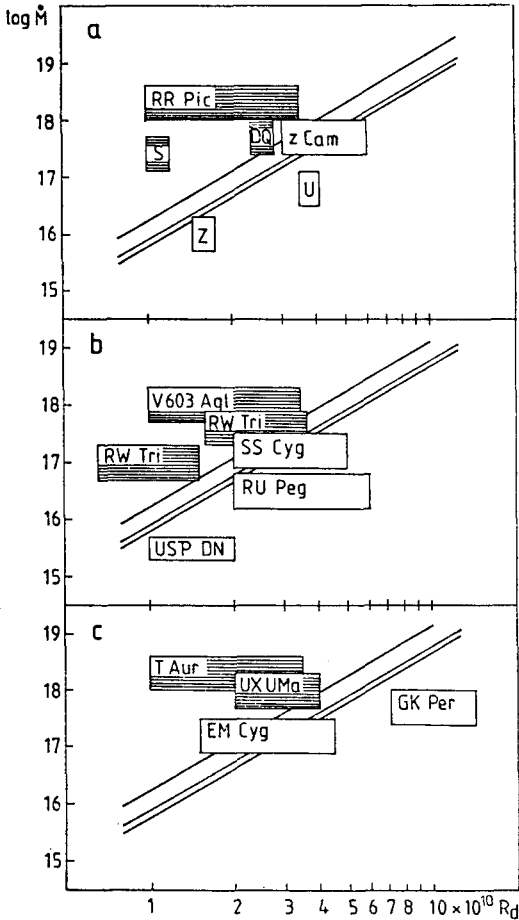


Fig. 5. \dot{M} - R diagram (from [17]). Theoretical border lines between stable and unstable disks for central masses 0.5, 1, and $1.2 M_{\odot}$ (from top). Shaded: novae and novae like, open: dwarf novae. DQ = DQ Her, U = U Gem, Z = Z Cha, S = Stepanyan's star

The curve $f(\Sigma)$ describes the states of thermal equilibrium in the disk where heat generation by friction and heat loss by radiation are in balance. It therefore separates the region of unbalance where either gains or losses dominate. Since large surface densities tend to impede the radiative heat losses non-equilibrium disks to the the right of the separating $f(\Sigma)$ line heat up, to the left cool down. Therefore their effective temperature (or their viscosity integral) increases to the

right and decreases to the left of the f - Σ curve on the thermal timescale. Is the radial scale length of the disturbance large compared to the vertical scale height the surface density cannot change on such short a timescale. Non-equilibrium disks will therefore perform paths in the f - Σ diagram that move vertically up on the right side and vertically down on the left side. Thus the upper hot and the lower cool branches of the disk structure with $\partial f/\partial \Sigma > 0$ are also thermally stable, the middle branch $\partial f/\partial \Sigma < 0$ is also thermally unstable.

Within the short thermal timescale the disk must always relax to one of the two stable branches. For mass accretion rates \dot{M}_b fed into the disk by the secondary star which lie between \dot{M}_A and \dot{M}_B no stable stationary solution exists. If the disk would initially be on the cool lower branch the local mass flow rate \dot{M} is too small and surface density must accumulate until the critical value Σ_B is reached. Any further increase of surface density must then lead to a rapid (thermal) transition to the only existing hot radiative state. On that branch the local mass flow rate \dot{M} exceeds the feeding rate \dot{M}_b , the surface density depletes until at Σ_A a transition back to the cool state ensues. Disk regions whose local $f(\Sigma, r)$ curves only allow unstable stationary solutions for the given \dot{M}_b thus perform limit cycles with a longer time interval (low diffusivity) of surface density built-up followed by a shorter time interval (high diffusivity) of depletion of the accumulated mass.

Cyclic quiescence-outburst behaviour of disks in this manner was suggested as the cause of dwarf novae outbursts (HOSHI [18], MEYER and MEYER-HOFMEISTER [19,20], SMAK [21], CANNIZZO, GOSH and WHEELER [22]) after Osaki [17] had shown that a disk instability of then unknown origin could yield a viable model for dwarf novae outbursts.

Figure 5 from SMAK [23] is an observational test of this theory. Above the critical lines $M-R_d$ (disk radius) an accretion disk everywhere is too hot to show effects of partial ionization and should not show outbursts. The observed cataclysmic systems are clearly divided by these critical lines into stationary UX Uma and post novae above and dwarf novae below.

The conservation equations (5), (6) do not allow a stationary transition between a hot and a cold state in such bi-stable regions of the disk. The continuous distribution of the friction f between a low value on one side and a high value on the other side of a boundary between two disk regions in different states must therefore necessarily involve a motion of such a boundary, i.e. a moving transition front. Such fronts are a new phenomenon in accretion disk theory which appears together with the bi-stable regions. Their thickness Δr and velocity of propagation V_F can be estimated by equating the viscous timescale $(\Delta r)^2/\nu$ to the thermal timescale t_{th} and equating the thickness Δr to the distance $V_F t_{th}$ covered in the transition time. This is analogous to the procedure for combustion waves and yields with the values of ν and t_{th} (16) and (18)

$$\Delta r \approx H \quad (23a)$$

and

$$V_F \approx \alpha \Omega H \approx \alpha V_g \quad (23b)$$

Transition fronts thus are thin and move across the disk on a timescale

$$t_F \approx \frac{r}{V_F} \quad (24)$$

which lies between that of radial diffusion and that of thermal relaxation,

$$\left(\frac{H}{r}\right)^2 t_d \approx \frac{H}{r} t_F \approx t_{th} \quad (25)$$

Both kinds of transition waves occur, those in which the material transits from a

cold to the hot state ("heating wave") and the reverse type ("cooling wave"). Once gas in the cool state at same distance r has accumulated critical density Σ_B and locally transits to the hot state, transition waves spread out through the bi-stable region transforming the cool state of a whole disk region into the hot state. In this state the viscosity is considerably higher than in the cool state before, resulting in the onset of rapid mass diffusion toward the central star and the corresponding steep increase in accretion luminosity. Transition waves thus provide the spatial and temporal coherence of the outbursts.

One problem that arises here is the following. Since transition fronts can propagate only inside the bi-stable region they must be reflected at the boundaries of these regions as a transition wave of the opposite type. Thus an outward moving heating wave on reaching the outer boundary $\Sigma = \Sigma_A(r)$ will be reflected as an inward moving cooling wave. Since these waves typically travel by a factor r/H faster than the diffusive mass flow they will leave the latter little time to develop in the hot state before the cool state is restored by a cooling wave. Since little mass has flown the next "ignition" to the hot state will also occur soon and one thus obtains a rapid sequence of small amplitude light variations quite distinct from the observed large amplitude outbursts with their long time of quiescence. The situation is also not made better if the outer disk rim still lies completely in the bi-stable region, since the relaxation cycle itself will lower the boundary value of Σ there to a value very near to the critical density Σ_A . The source of this problem is the rather fast propagation of the cooling front.

Analysis of this situation has led to the suggestion that α may not be constant but may depend on the other locally defined non-dimensional number H/r . Such a dependence must in general be expected for any physical model of the not yet specified viscosity. A small scale magnetic dynamo acting in the disk could eg. display a $\alpha \sim (H/r)^{3/2}$ relation ([24]). This will lead to cooling transition waves sufficiently slow to result in larger amplitude outbursts. Model outburst calculations by Smak [25] and by Mineshige & Osaki [26] have also indicated that α should be smaller in the cool convective disk state than in the hot radiative state.

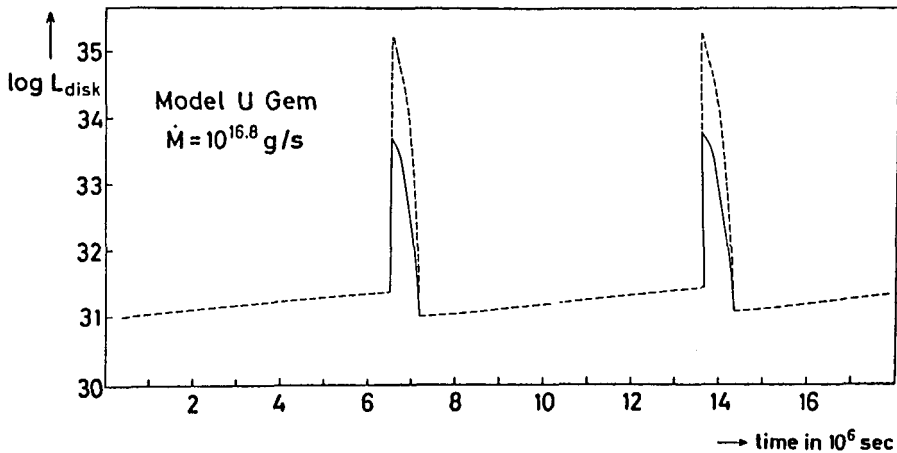


Fig. 6. Visual and bolometric (dashed) light curves for U Gem model (from [25])

Various groups have performed disk outburst calculations, mostly by solving the diffusion equation together with the thermal equation ([27,28,29,26,25]). Since the latter introduces the short thermal timescale t_{th} one is forced to small time steps and a large number of spatial points in order to resolve the spatial scale of order H in transition fronts. In practice some compromise between computing requirements and resolution has been made. Alternatively one may fully resolve the transition fronts in a local quasi-stationary approximation and solve for the thermally relaxed regions by the diffusion equation only [30,31]. Figure 6 shows the result of such computations.

Low mass X-ray binaries are similar systems, only the white dwarf is replaced by a neutron star of similar mass. Why do they not show corresponding outburst cycles? The neutron star liberates about 10^3 times more accretion light than the white dwarf due to its 10^3 times smaller radius. This strongly irradiates the disk and affects its thermal structure. The convective outer disk regions lie in the shadow of interior radiative regions with higher z_0/r but indirect irradiation from the central source can still reach these regions by reflection at the secondary's surface and scattering in the disk's corona. Estimates indicate an irradiation flux that would heat a black body surface to 6000K to 8000K [32].

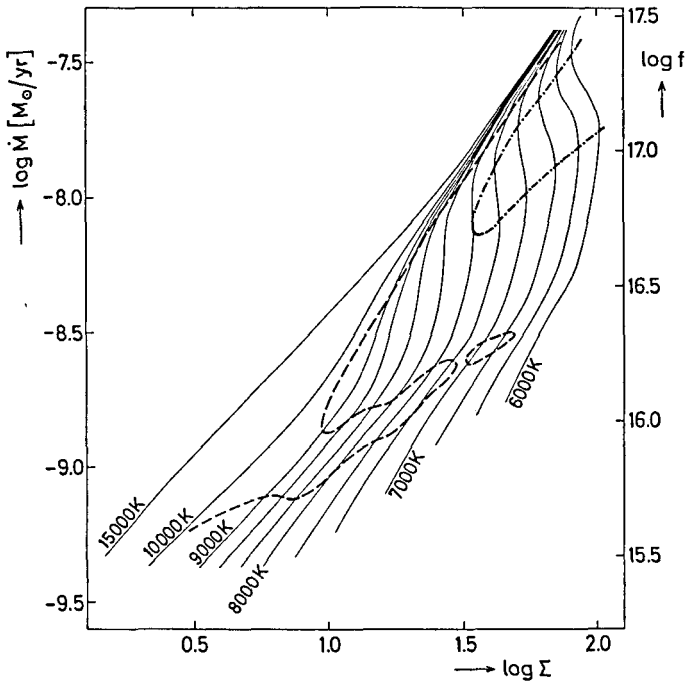


Fig. 7. Viscosity-surface density diagram at $\log r = 11$ for various "irradiation temperatures". Regions between dashed and dashed-dotted lines are thermally stable but diffusively unstable ([32])

This contributes a significant part to the local heat release and is able to stabilize the thermal instability since the unstable influence of friction on the local

structure is weakened. Figure 7 shows this stabilizing influence as a flattening of the S-shaped f - Σ curves. The diffusive instability of the radial disk structure can, however, not be fully removed: On long timescales the central accretion rate follows the mass accretion rate of the outer regions. Disk structure and irradiation vary together. This can lead to self-excited non-linear mass flow variations with periods of the order of the radial diffusion time from the unstable region to the center. Figure 8 shows results from model calculations [32]. Long-term variations with periods ranging from 40 to 200 days were discovered for several galactic X-ray sources by Priedorsky and Terrell [33,34].

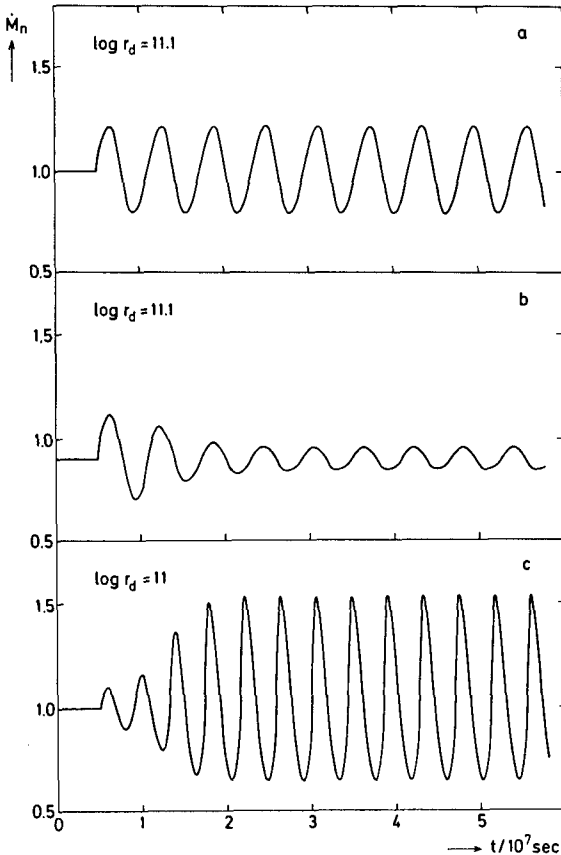


Fig. 8. On-set of non-linear self-excited mass flow variations in self-irradiated accretion disks around neutron stars for various disk radii r_D in cm. Mean mass accretion rates in units of $3 \cdot 10^{-9} M_{\odot}/\text{yr}$ [from 32]

IV. The Lightman-Eardley Instability

1974 Lightman and Eardley [1] discovered that stationary α disks become unstable when electron scattering opacity dominates and the ratio of gas pressure to total

pressure falls below 2/5. This situation is expected in interior parts of accretion disks around neutron stars depending on the mass accretion rate

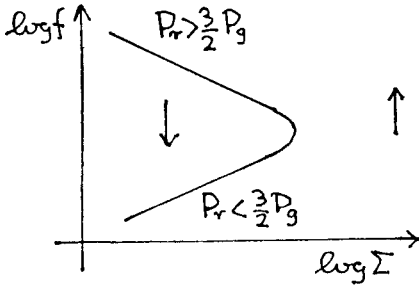


Fig. 9. Schematic viscosity–surface density diagram when radiation pressure P_r becomes important. Arrows indicate direction of thermal relaxation. Upper branch $P_r > \frac{3}{2}P_g$ is unstable

Figure 9 shows schematically the viscosity–surface density relation. The upper branch $df/d\Sigma < 0$ is unstable diffusively [1] and (on the same argument as given in section II) also thermally [35,36].

In the following we discuss how this instability is removed when the coupling of the friction is to the gas pressure instead of to the total pressure (as in models of magnetic friction) and α is constant [1], but that the instability reappears when α becomes a sufficiently strong function of H/r . For the rapid burster there are indications that the latter may be the case. We limit ourselves to the thermal instability (the diffusive radial instability goes parallel to it) for constant electron scattering opacity κ .

Radiative energy transport from the interior of the disk to its surface gives the local energy loss to each side as

$$F_r = - \frac{4acT^3}{3\kappa\rho} \frac{dT}{dz} \approx \frac{2}{3} \frac{acT^4}{\kappa\Sigma} \tag{26}$$

(a a radiation constant, c speed of light). This must stationary be in balance with the local energy gain by friction

$$F_f = \int_0^\infty \mu \left[\frac{d\Omega}{dr} \right]^2 dz \approx \frac{9}{4} \mu \Omega^2 H \approx \frac{3}{2} \alpha H \Omega P \tag{27}$$

(For "magnetic friction" P is to be replaced by P_g in the last term.) The scale height is given by hydrostatic vertical equilibrium,

$$H^2 \approx \frac{2P}{\rho\Omega^2} \tag{28}$$

This becomes for dominating gas pressure

$$H \approx (2P_g T)^{1/2} / \Omega, \quad P_g \gg P_r \tag{28a}$$

and for dominating radiation pressure

$$H \approx 4aT^4 / (3\Sigma\Omega^2), \quad P_g \ll P_r \tag{28b}$$

In equilibrium the ratio $q \equiv F_r / F_f = q(T)$ is $q=1$. If a variation in local temperature results in frictional heat gains becoming larger than radiative losses, $\delta q / \delta T < 0$ the

disk heats up even more and is unstable [36].

Thus when friction is proportional to the *total* pressure, $\tau_{r\phi} = \alpha P$, the two limiting cases become ((26) to (28))

$$P_g \gg P_r \quad q = \frac{8\alpha c T^3}{9\alpha\kappa\Sigma^2\Omega R_g} \quad \frac{\delta q}{\delta T} > 0 \text{ stable} \quad (29a)$$

$$P_g \ll P_r \quad q = \frac{c\Omega}{3\alpha\kappa a T^4} \quad \frac{\delta q}{\delta T} < 0 \text{ unstable.} \quad (29b)$$

On the other hand, when friction is proportional to the *gas pressure* only, $\tau_{r\phi} = \alpha P_g$, one obtains instead of the latter equation the same relation as in (29a),

$$P_g \ll P_r \quad q = \frac{8\alpha c T^3}{9\alpha\kappa^2 \Omega R_g} \quad \frac{\delta q}{\delta T} > 0 \text{ stable.} \quad (29c)$$

thus stabilizing the Lightman-Eardley instability.

The above considerations hold when α is constant. If, however, α depends on the ratio (H/r) , e.g.

$$\alpha = \alpha_0 \left[\frac{H}{r} \right]^n \quad (30)$$

then even for friction coupled to the gas pressure one has (see (29c) and (30))

$$P_g \ll P_r \quad q \sim \frac{T^3}{\alpha} \sim T^{3-4n} \quad (31)$$

and accordingly

$$\frac{\delta q}{\delta T} > 0 \text{ for } n < \frac{3}{4} \text{ stable.} \quad (31a)$$

$$\frac{\delta q}{\delta T} < 0 \text{ for } n > \frac{3}{4} \text{ unstable.} \quad (31b)$$

Thus an α -dependence with $n > 3/4$ reintroduces the Lightman-Eardley instability. We suggest in the following section that this instability is intimately involved in the type II bursts of the rapid burster MXB 17030-335.

V. Type II Bursts of the Rapid Burster and the Lightman-Eardley Instability

The viscosity-surface density relation of the Lightman-Eardley instability (Fig. 9) does not show an upper stable branch, in contrast to the S-shaped curves of the instability related to partial ionization discussed in section III (Fig. 4). Thus one must conclude that under ideal circumstances the disk must unrestrictedly expand on the thermal timescale once locally the Lightman-Eardley stability limit $P_g = 2P/5$ is reached. This expansion is only ended when a more or less spherical configuration around the neutron star is reached. Then thin disk equations no longer apply and radial pressure support and radial heat transport are no longer negligible.

Which part of the accretion disk will be thus transformed once the instability is triggered at some interior point r_{LE} ? As was the case for dwarf novae outbursts transition waves will propagate inward and outward transforming gas pressure supported regions into a hot thick radiation supported spherical structure. Since inside the front of thickness H the local surface density must first be raised to the local critical value Σ_c (compare Fig. 9) such a front incorporates a mass of order

$$(\Delta M)_F \approx 2\pi r (\Sigma_c - \Sigma) H. \quad (32)$$

This value increases with r as stationary disk models show and finally becomes even more than the total disk mass within r , before which point the transition must come to an end. This limits the transformed region to some multiple of r_{LE} .

One may estimate the critical radius r_{LE} as the distance in which a stationary gas pressure supported disk has a radiation pressure equal to the gas pressure. This yields

$$r_{LE} \approx 10^{8.6} (\dot{M}_{18})^{16/21} \alpha^{2/21} \text{ cm} \quad (33)$$

where \dot{M}_{18} is the mass accretion rate in 10^{18} g/s. The mass involved in the outburst is then of order

$$\Delta M \approx (\pi r^2 \Sigma)_{LE} \approx 10^{20.8} (\dot{M}_{18})^{5/3} \alpha^{1/3} \text{ g}. \quad (34)$$

The thermal rise time at that distance comes out as

$$t_{LE} \approx 10^{-0.2} (\dot{M}_{18})^{8/7} \alpha^{-6/7} \text{ s}. \quad (35)$$

The time for the transition wave to transform the whole inner region is by about a factor $r/H \approx 30$ larger.

$$t_F \approx 10^{1.2} (\dot{M}_{18})^{8/7} \alpha^{-6/7}. \quad (36)$$

For $\alpha=1/3$ and $\dot{M}_{18}=1$ this takes about 40 seconds. On this time scale the thickening disk will obscure the central light source at the beginning of an outburst. This compares favourably to dips in the persistent emission from the rapid burster observed before and after several type II bursts from the rapid burster by Kunieda et al. [4] starting 30 to 60 s before the outburst and recovering about 1 min after the end of the burst.

Next we consider the expected fate of the region made spherical (Fig. 10). Differential rotation will relax on the dynamical time scale to a more or less solid

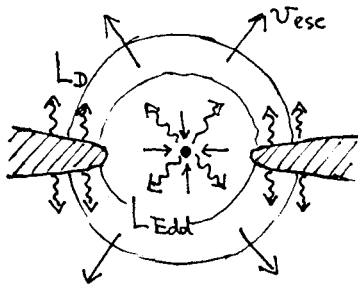


Fig. 10. The spherical inner region is mainly supported by "near Eddington" luminosity. The additional disk luminosity L_D lifts outer material to infinity

body rotation. Also on this time scale convective exchanges redistribute the mass in the new configuration. Since rotation is no longer critical the matter will centrally accrete until it can be supported by gas pressure gradients and a luminosity near the Eddington value. This is similar to the central parts of stars containing a neutron star core (THORNE and ZYTKOW [37]). Equilibrium requires

$$\frac{dP_g}{dr} = -\rho \frac{GM}{r^2} \left(1 - \frac{L}{L_{\text{Edd}}}\right) \quad (37)$$

Such models reach optical depth ρkr unity at about $r=10^{7.6}$ cm. With a temperature of $T \approx 10^{7.3}$ K one can estimate from (37) at this point a typical value

$$\frac{\Delta L}{L_{\text{Edd}}} = \frac{L_{\text{Edd}} - L}{L_{\text{Edd}}} \approx 10^{-3.4} \quad (38)$$

with $L_{\text{Edd}} = 4\pi GMc/\kappa \approx 10^{38.2}$ erg/s.

To this is added the accretion luminosity of the remaining disk estimated by

$$L_D \approx \frac{GM}{r_{\text{LE}}} \dot{M} \quad (39)$$

which yields for $\dot{M}_{18}=1$, $r_{\text{LE}}=10^{8.6}$ cm about $10^{-2.5} L_{\text{Edd}}$. Thus for r_{LE} the combined luminosity is more than the Eddington value and the gas will "fall" outward under an effective gravity

$$g_{\text{eff}} = -\frac{GM}{r^2} \left(1 - \frac{L + L_D}{L_{\text{Edd}}}\right) \approx \frac{GM}{r^2} \frac{L_D}{L_{\text{Edd}}} \quad (40)$$

and disperse on the "free-fall" time

$$t_B \approx \frac{1}{\Omega(r_E)} \sqrt{\frac{L_{\text{Edd}}}{L_D}} = \frac{1}{\Omega} \sqrt{\frac{4\pi r_{\text{LE}}^3}{\kappa \dot{M}}} \quad (41)$$

During this time the accretion luminosity is about L_{Edd} . This gives the total burst energy as

$$E_B \approx L_{\text{Edd}} t_B \quad (42)$$

One can relate this to the time t_q between consecutive bursts (during which the evaporated mass ΔM (34) must be replaced in the disk),

$$t_q \approx \Delta M / \dot{M} \quad (43)$$

Elimination of \dot{M} between E_B and t_q gives the expected correlation that is caused by secular changes of the mean mass accretion rate. This yields

a) $\alpha = \text{const.}$

$$\log E_B = 35.1 - \frac{5}{6} \log \alpha + 1.53 \log t_q \quad (44a)$$

The observed slope is about 1.33 (see Fig. 11). In order to fit the burst energy at large t_q $\log \alpha$ would have to be -0.84 . A better fit is obtained for

b) $\alpha = \alpha_0 (H/r)^n$ with $n = 3/2$ and $\alpha_0 = 50$

$$\log E_B = 35.6 + 1.4 \log t_q \quad (44b)$$

This is the same α prescription (derived from a small scale magnetic dynamo consideration) that gave reasonable model dwarf novae outbursts. For $\log t_q = 2.8$ this gives $\log E_B = 39.5$ (observed ≈ 40.2)

c) $\alpha = \alpha_0 (H/r)^n$ with $n = 3$, $\log \alpha_0 = 3.9$

$$\log E_B = 37.0 + 1.33 \log t_q \quad (44c)$$

Here the value of α_0 was chosen such that the values of α are in the same range as before (as required by dwarf novae observations). Cases (b) and (c) both represent quite well the observed $E_B - t_q$ correlation (Fig. 11). Had the mass loss driven by radiation of the remaining disk been neglected a quite different correlation would have been obtained.

$$\log E_B = \text{const} + 2.5 \log t_q .$$

It should be noted that these correlations are those resulting from secular (long-term) variations of the mean accretion rate. Even if this rate is constant there will be fluctuations in burst energies and time of quiescence since the disk instability will not be strictly periodic. The transformation fronts will propagate not always exactly to the same radial distance and the following disk relaxation will not lead to exactly the same disk state when the next burst is triggered. Such fluctuations also occur in dwarf novae outburst simulations and may be responsible for the other observed correlation that for short-time periods (when presumably the mean accretion rate stays constant) individual burst energies vary like $\log E_B \propto \text{const} + \log t_q$ [38.4].

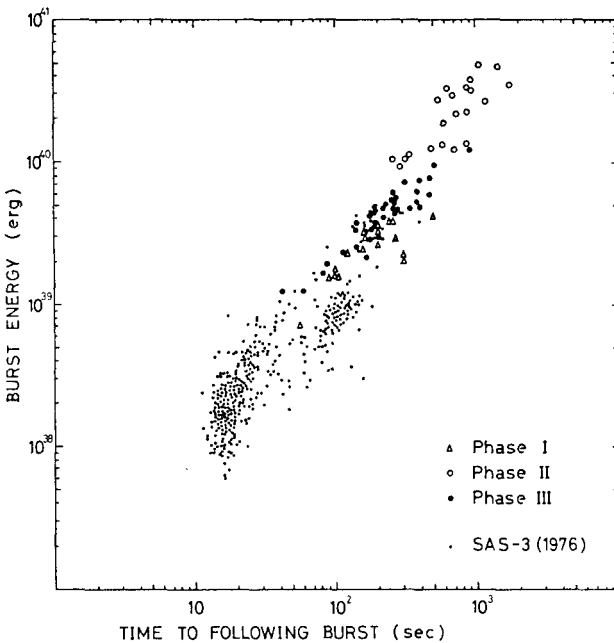


Fig. 11. Observed relation between the burst energy and the time to the following burst for type II bursts of the rapid burster (from KUNIEDA et al. [4])

The rapid burster thus appears unique in that its mean mass accretion rate \dot{M} stays below the Eddington critical value of $\approx 10^{18}$ g/s and can thus not support a steady more or less spherical accretion close to the neutron star (as presumably all the other high luminosity sources do, $M_B \geq 1$). It therefore must alternate between bursts at Eddington luminosity (the trapezoidal bursts) and inner disk recovery. A further consistency is the relation

$$\log t_q = 2.8 + 1/3 \log \alpha + 2/3 \log \dot{M}_B \quad (45)$$

following from (34) and (43). The longest trapezoidal bursts, $\log t_{\text{tr}} \approx 2.8$, thus limit the accretion rate to values $M_{\text{tr}} \leq (1/\nu\alpha)$ near the Eddington limit $M_{\text{Edd}} = 4\pi R c / \kappa$.

An important objection was raised during the conference by Ebisuzaki: Type I bursts (presumably thermonuclear) of the rapid burster reach counting rates above the level for type II trapezoidal bursts. Since in these type I bursts there is no apparent mass loss their luminosity should not exceed the Eddington value. Also theoretical models indicate sub-Eddington values for type I bursts [39]. We cannot go here into details of the discussion for over-Eddington luminosities, but mention the possibility that dynamo-created fields from the convection caused by the thermonuclear burst carry a significant part of the energy magnetically to the surface and release it in the atmosphere, presumably as relativistic particles bombarding the photosphere from above and keeping it confined. Then super-Eddington luminosities can result without dynamic appearance. (This could also relieve the distance problem for the bulge sources in the galactic center). Further the radiation flux of the type II bursts could appear sub-Eddington if part of it has been transformed into kinetic energy of outward accelerated mass flow by optically deep expansion.

Two other observations seem to naturally fit into the model discussed in this section. One is the remarkable time scale invariant decay profile of type II bursts reported by Tanaka in this conference. Scaled with the individual characteristic decay time scale t_c (ranging from 10 seconds down to fractions of a second) the temporal decay $F(t/t_c)$ of the burst in form of a series of peaks of decaying amplitude and decreasing time separation appears always the same. We suggest here that this is a consequence of the decrease of density by mass loss of the spherical burst configuration. If at the end of the burst this density becomes too low the accretion flow velocity must increase to keep the accretion luminosity near critical but will become too high to allow the angular momentum to be transported outward. Then radial infall will be stopped by angular momentum and the rest density will settle into a rotation supported disk structure now inside and presumably will separated from the outer rebuilding accretion disk. This disk must still be expected to repeatedly become Lightman-Eardley unstable, but on decreasingly shorter time scales and with decreasingly smaller energies as its mass drains in a succession of instabilities toward the neutron star. This process would be very similar to the results of Taam and Lin [40], who obtained a periodic sequence of bursts for smaller steady accretion rates (in which the disk never became fully inflated due to effects of radial heat conduction) except that in the present case the mass accretion rate would decrease due to the decreasing disk size. The work by these two authors independently had already suggested a relation between the Lightman-Eardley instability and the type II bursts.

A second observation that became known to the author after the end of the conference and that is to be noted in this context is the reported appearance of quasiperiodic oscillations (QPO's) in a number of high luminosity bulge sources (see e.g. [41] and the rapid burster (L. Stella, private communication). It will be natural to attribute these to oscillations excited in the spherical accretion region around the neutron stars. Such a model when worked out might provide an important diagnostic tool for the accretion process in the rapid burster and the other bright galactic X-ray sources.

The two accretion disk instabilities discussed in this article are only examples from a much wider area in which high energy accretion and disks play an essential role. This includes such diverse objects as symbiotic stars, the galactic supernova remnant SS433, possibly the gamma burst sources, disks around young or still forming stars, and disks in the nuclei of active galaxies, giant radio galaxies, and quasars. Many of these objects show time variations in their light, often dramatic, which may be related to corresponding variations of the mass accretion rates in their disks. One may expect still further interesting progress in our understanding of these objects by future theoretical and observational work on the physics of these

accretion processes.

References

1. A.P. Lightman and D.M. Eardley: *Astrophys. J. Lett.* **187**, L1 (1974)
2. J.S. Glasby: "The Dwarf Novae", Constable Co. Ltd. London, p. 201 (1970)
3. W.H.G. Lewin, J. Doty, G.W. Clark, S.A. Rappaport, H.V.D. Bradt, R. Duxsey, D.R. Hearn, J.A. Hoffman, J.G. Jernigan, F.K. Li, W. Mayer, J. McClintock, F. Primi and J. Richardson: *Astrophys. J. Lett.* **207**, L95 (1976)
4. H. Kunieda, Y. Tawara, S. Hayakawa, K. Masai, F. Nagase, H. Inoue, K. Koyama, F. Makino, K. Makishima, M. Matsuoka, T. Murakami, M. Oda, Y. Ogawara, T. Ohashi, N. Shibazaki, Y. Tanaka, I. Kondo, S. Miyamoto, H. Tsunemi, and K. Yamashita: *Publ. Astron. Soc. Japan* **36**, 215 (1984)
5. J.E. Pringle: *Ann. Rev. Astron. Astrophys.* **19**, 137 (1981)
6. J. Smak: *Publ. Astron. Soc. Pacific* **96**, 5 (1984)
7. F. Meyer: in "Recent Results on Cataclysmic Variables", Proceedings of an ESA Workshop in Bamberg, W.R. Burke ed., ESA sp-236, ESTEC, Noordwijk, p. 83 (1985)
8. N.I. Shakura and R.A. Sunyaev: *Astron Astrophys.* **24**, 337 (1973)
9. I.D. Novikov and K.S. Thorne: in "Black Holes", C. DeWitt, B.S. DeWitt eds., Gordon & Breach, New York (1973)
10. G.T. Bath and J.E. Pringle: *Mon. Not. Roy. astron. Soc.* **194**, 967 (1981)
11. W.J. Duschl: *Astron. Astrophys.* **119**, 248 (1983)
12. R.E. Williams: *Astrophys. J.* **235**, 939 (1980)
13. R. Tytenda: *Acta Astron.* **31**, 127 (1981)
14. F. Meyer and E. Meyer-Hofmeister: *Astron. Astrophys.* **106**, 34 (1982)
15. W.J. Duschl: *Astron. Astrophys.* **121**, 153 (1983)
16. G.T. Bath and J.E. Pringle: *Mon. Not. Roy. astron. Soc.* **199**, 267, (1982)
17. Y. Osaki: *Publ. Astron. Soc. Japan* **26**, 429 (1974)
18. R. Hoshi: *Prog. Theor. Physics* **61**, 1307 (1979)
19. F. Meyer and E. Meyer-Hofmeister: *Astron. Astrophys.* **104**, L10 (1981)
20. F. Meyer and E. Meyer-Hofmeister: *Astron. Astrophys.* **126**, 34 (1982)
21. J. Smak: *Acta Astron.* **32**, 199 (1982)
22. J. K. Cannizzo, P. Gosh, and J.C. Wheeler: *Astrophys. J. (Letters)* **260**, L83 (1982)
23. J. Smak: *Acta Astron.* **32**, 213 (1982)
24. F. Meyer and E. Meyer-Hofmeister: *Astron. Astrophys.* **128**, 420 (1983)
25. J. Smak: *Acta Astron.* **34**, 161 (1984)
26. S. Mineshige and Y. Osaki: *Publ. Astron. Soc. Japan* **35**, 3 (1983)
27. J. Papaloizou, J. Faulkner, and D.N.C. Lin: *Mon. Not. Roy. astron. Soc.* **205**, 487 (1983)
28. D.N.C. Lin, J. Papaloizou, and J. Faulkner: *Mon. Not. Roy. astron. Soc.* **212**, 105 (1985)
29. S. Mineshige and Y. Osaki: *Publ. Astron. Soc. Japan* **35**, 377 (1983)
30. F. Meyer: *Astron. Astrophys.* **131**, 303 (1984)
31. F. Meyer and E. Meyer-Hofmeister: *Astron. Astrophys.* **132**, 143 (1984)
32. F. Meyer and E. Meyer-Hofmeister: *Astron. Astrophys.* **140**, L35 (1984)
33. W.C. Priedhorsky and J. Terrell: *Astrophys. J.* **280**, 661 (1984)
34. W. Priedhorsky and J. Terrell: *Astrophys. J. (Letters)* **284**, L17 (1984)
35. N.I. Shakura and R.A. Sunyaev: *Mon. Not. Roy. astron. Soc.* **175**, 613 (1976)
36. J.E. Pringle: *Mon. Not. Roy. astron. Soc.* **177**, 65 (1976)
37. K.S. Thorne and A.N. Zytkov: *Astrophys. J.* **212**, 832 (1977)
38. W.G. Lewin and P.C. Joss: *Space Science Rev.* **28**, 3 (1981)
39. T. Ebisuzaki, T. Hanawa, and D. Sugimoto: *Publ. Astron. Soc. Japan.* **36**, 551 (1984)
40. R.E. Taam and D.N.C. Lin: *Astrophys. J.* **287**, 761 (1984)
41. M. van der Klis, F. Jansen, J. van Paradijs, W.H.G. Lewin, E.P.J. van den Heuvel, J.E. Trümper, and M. Sztajno: *Nature* **316**, 225 (1985)